

Elastic and charge transfer cross sections for low to ultralow $\text{H}(1s) + \text{H}^+$ collisions. Quantal and semiclassical calculations

Mykhaylo Khoma^{1,2*}

^{1*}Max Planck Institute for the Physics of Complex Systems, Nöthnitzer Str. 38, Dresden, 01187, Germany.

²Institute of Electron Physics, National Academy of Sciences of Ukraine, Universytetska Str. 21, Uzhhorod, 88017, Ukraine.

Corresponding author(s). E-mail(s): khomamv@nas.gov.ua;

Abstract

The elastic scattering and resonant charge transfer integral cross sections in $\text{H}(1s) + \text{H}^+$ collisions are computed for the center-of-mass energy range of $10^{-10} - 10$ eV. Fully quantal and semiclassical approaches are utilized in these calculations. The reliability of the semiclassical approximation for very low collision energies is discussed. The results are compared with available data from the literature.

Keywords: Slow ion-atomic collisions, elastic scattering, charge transfer, semiclassical approximation

1 Introduction

The elementary processes occurring during proton impact on atomic hydrogen are important for many applications such as astrophysical and fusion plasmas [1–8], and have thus been a subject of active study for many decades [9–16].

The fundamental quantum mechanical methods used to calculate the elastic and charge transfer cross sections for proton-hydrogen collisions in the low energy regime have been described in detail (see [9–13] and references therein). These methods are based on the extraction of the phase shifts from the numerical propagation of the corresponding radial Schrödinger equation (or system of equations) to sufficiently

large distances between the scattering particles. Having the phase shifts, the total or differential cross-sections can be computed in the standard manner [11–14].

An alternative method which addresses the problem of the symmetric ion-atomic collisions is via the semiclassical computation of the scattering phases [16–18]. It is well known that the standard semiclassical approximations works reasonably well for intermediate and high collision energies. At low and very low collision energies, the so-called orbiting resonance phenomena may occur due to the possibility of formation and decay of the collision complex through trapping by the attractive polarisation force between the colliding particles [19]. A more involved version (with three classical turning points) of the semiclassical theory exists to treat this case [20, 21]. Surprisingly, only a few works have directly applied this theory for computation of the cross sections in the presence of orbiting resonances [19, 22].

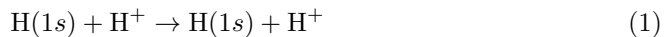
In this paper, we present detailed calculations of the phase shifts and the total cross sections for elastic scattering and charge transfer for symmetric $\text{H}(1s) + \text{H}^+$ collision by means of fully quantal and semiclassical approaches. Numerical results are presented for the energy range of $10^{-10} \leq E_{\text{c.m.}} \leq 10$ eV. Here $E_{\text{c.m.}}$ is the collision energy in the center-of-mass frame. Finally, one of the goals of present work is to study the reliability of the semiclassical approach to ultra-low collision energies.

The article is organized as follows. In section 2, we briefly summarize the most relevant aspects of the theoretical approaches. The numerical details of the phase shift computations are also given in this section. In section 3, we present the results of the cross section calculations. The final discussion and concluding remarks are given in section 4.

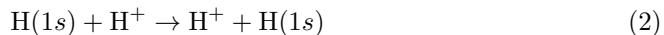
Throughout this paper we use atomic units (a.u.) for all quantities. For the sake of concreteness, we adopt the following energy conversion factor between a.u. and eV: $\text{eV}/27.211386$ [23].

2 Theory

We compute the cross sections for elastic scattering (EL)



and for resonant charge transfer (CT)



for proton collision with atomic hydrogen using quantum mechanical and semiclassical methods.

For the energy range considered here, only two lowest electronic states of H_2^+ , the $1s\sigma_g$ *gerade* (g) and $2p\sigma_u$ *ungerade* (u), are involved. Thus, the cross sections for reactions (1) and (2) may be obtained from solutions of uncoupled single-channel Schrödinger equations (see, e.g. [4–7]) of the form

$$\left(\frac{d^2}{dR^2} + k^2 - 2\mu V_{g,u}^{(l)}(R) \right) \psi_{g,u}^{(l)}(R) = 0, \quad (3)$$

where $k^2 = 2\mu E_{c.m.}$, μ is the system reduced mass, l is the orbital angular momentum of the collision system, R is the internuclear distance, $V_{g,u}^{(l)}(R)$ is the adiabatic potential for either the $1s\sigma_g$ or $2p\sigma_u$ electronic state, and $\psi_{g,u}^{(l)}(R)$ is the radial wave function for the corresponding reaction channel. The adiabatic potential $V_{g,u}^{(l)}(R)$ reads

$$V_{g,u}^{(l)}(R) = E_{g,u}^{\text{BO}}(R) + \frac{l(l+1)}{2\mu R^2}, \quad (4)$$

where $E_{g,u}^{\text{BO}}(R)$ is the Born-Oppenheimer (BO) potential energy curve (PEC) of the corresponding electronic state. For the purpose of the present study we calculated the BO PECs for $1s\sigma_g$ and $2p\sigma_u$ states of the H_2^+ system to very high accuracy (~ 28 - 30 decimals) for a wide range of the distance R ($0 < R < 10^4$ a.u.) by using a quadruple precision arithmetics and the algorithm described in [1]. We set the zero of energy at the asymptote of the BO PECs (i.e. $\lim_{R \rightarrow \infty} V_{g,u}^{(l)}(R) = 0$), so the asymptotic form of the radial wave functions $\psi_{g,u}^{(l)}(R)$ reads [24]

$$\psi_{g,u}^{(l)}(R)|_{R \rightarrow \infty} \simeq \sin(kR + \delta_{g,u}(l) - \pi l/2), \quad (5)$$

where $\delta_g(l)$ and $\delta_u(l)$ are the scattering phase shifts.

2.1 Semiclassical calculation

For not very low collision energies, the semiclassical (JWKB) approach can be used for computation of the scattering phase shifts [13, 17]. The 'classical' (single turning point R_0) JWKB approach provides the following expression for the phases $\delta_{g,u}(l)$

$$\delta_{g,u}(l) = \int_{R_0}^{\infty} (k_l(R) - k) dR - kR_0 + \frac{\pi}{2} \left(l + \frac{1}{2} \right), \quad (6)$$

where $k_l(R)$ is given by

$$k_l(R) = \sqrt{2\mu E_{c.m.} - 2\mu V_l^{\text{eff}}(R)}, \quad (7)$$

and $V_l^{\text{eff}}(R)$ is the effective potential including the Langer modification

$$V_l^{\text{eff}}(R) = E_{g,u}^{\text{BO}}(R) + \frac{(l+1/2)^2}{2\mu R^2}. \quad (8)$$

As mentioned earlier in the Introduction, for collision systems with an attractive potential there can be a considerable range of l values for which the effective radial potential $V_l^{\text{eff}}(R)$ has three classical turning points [20]. We find this phenomena occurs for $1s\sigma_g$ state at collision energies $E_{c.m.} \lesssim 0.017$ a.u.

To determine the semiclassical phase shifts for this case we follow the algorithm and notations adopted in [20, 21]. Assume that a_l , c_l , and e_l are the three classical

turning points (in the order of increasing of R value), and define the functions α_l and ε_l as

$$\alpha_l = \int_{a_l}^{c_l} k_l(R) dR, \quad (9)$$

$$\varepsilon_l = -\frac{1}{\pi} \int_{c_l}^{e_l} |k_l(R)| dR. \quad (10)$$

Then, the sought phase shift $\delta(l)$ reads

$$\delta(l) = \delta_0(l) - \frac{1}{2}\phi(\varepsilon_l) + \Theta(l), \quad (11)$$

where $\delta_0(l)$ is determined by expression (6), in which R_0 should be replaced by the outermost turning point e_l , the function $\phi(\varepsilon)$ is given by

$$\phi(\varepsilon) = \varepsilon + \arg \Gamma\left(\frac{1}{2} + i\varepsilon\right) - \varepsilon \ln |\varepsilon|, \quad (12)$$

with the phase correction $\Theta(l)$ defined as follows:

$$\Theta(l) = \arctan\left(\kappa(\varepsilon_l) \tan\left[\alpha_l - \frac{1}{2}\phi(\varepsilon_l)\right]\right), \quad (13)$$

$$\kappa(\varepsilon) = \frac{\sqrt{1 + \exp(2\pi\varepsilon)} - 1}{\sqrt{1 + \exp(2\pi\varepsilon)} + 1}. \quad (14)$$

The integration in (6) is carried out to sufficiently large R_{\max} . In all the semiclassical calculations presented here, we adopt $R_{\max} = 10^4$ a.u. This allows to achieve the convergence of 10^{-4} for all $\delta_{g,u}$.

In Table 1 we show the coordinates of a_l , c_l , and e_l for representative collision energies of 0.1 eV and 0.2 eV for all l for which there exists three turning points. The results of the semiclassical calculations of the phase shifts and cross sections will be presented further on.

2.2 Quantal calculation

One of the most widely used methods for quantal calculation of the scattering phase shifts consists of numerically integrating the radial equations (3) and matching the obtained solutions to the asymptotic form (5) (see, e.g., [9–11, 24–26]). In the present work, we use the approach described in [25, 26] to determine the phase shifts $\delta_{g,u}(l)$ at 1360 exponentially incremented energies between 10^{-10} eV and 10 eV. The energy points were chosen in order to resolve (as much as possible) the oscillating features of the integral cross sections. The standard Numerov's method was used to numerically integrate the radial equations (3) from $R_{\min}=0.001$ a.u. to $R_{\max}=1000$ a.u. with a stepsize of $R \sim 0.001$ a.u. In the lower energy regime, $E_{c.m.} \leq 10^{-6}$ eV, the value of R_{\max} was gradually increased from 5000 a.u. for $E_{c.m.} = 10^{-6}$ eV up to 6×10^4 a.u. for $E_{c.m.} = 10^{-10}$ eV. The choice of the largest orbital momentum l_{\max} depends on

Table 1 Coordinates (in a.u.) of the turning points a_l , c_l , and e_l for various l (see text for details) and representative energies $E_{c.m.}$ of 0.1 eV and 0.2 eV.

l	a_l	c_l	e_l
$E_{c.m.} = 0.1$ eV			
27	1.968459	7.667607	9.664132
28	2.040515	7.152738	10.346113
29	2.117967	6.778401	10.890103
30	2.201711	6.462717	11.376725
31	2.292953	6.178178	11.831895
32	2.393379	5.910682	12.267629
33	2.505459	5.650765	12.690516
34	2.633062	5.390169	13.104533
35	2.782893	5.119235	13.512236
36	2.968601	4.822214	13.915339
37	3.228774	4.458966	14.315023
$E_{c.m.} = 0.2$ eV			
34	2.549141	6.667577	8.328068
35	2.676997	6.108765	8.924692
36	2.825851	5.681096	9.373407
37	3.007278	5.284696	9.762399
38	3.250047	4.864168	10.118181
39	3.715295	4.246132	10.452863

the value of $E_{c.m.}$ and was similar to those adopted in [5]. Specifically, values of l_{\max} vary from 9 at 10^{-10} eV, 28 at 10^{-8} eV, and up to 1200 for 10 eV.

We find very good agreement in comparing our phase shifts with corresponding values tabulated in [9, 10]. The results are given in Table 2 for 0.1 and 10 eV for representative partial waves l . The integral cross sections for the reactions (1) and (2) are then computed from the phase shifts.

A note should be added concerning the definitions of elastic scattering and charge transfer for low-energy collisions involving identical nuclei as in the present case (a detailed discussion on this issue can be found in [9–14]). In view of quantum indistinguishability of identical particles (QIP) the elastic scattering and charge transfer can only be differentiated by using a nuclear spin for labeling. Consequently, in the QIP approach the charge transfer is termed as spin exchange [7, 9–14]. In this approach, the elastic scattering cross section contains the contributions both from the forward (elastic) and from the backward (charge transfer) scattering. With increase of collision energy the classical distinguishability of particles (CDP) becomes enabled, and so the elastic scattering and charge transfer processes can be separated out. Owing to the substantial interference of the direct and exchange scattering amplitude, the EL cross section in the QIP approach $\sigma_{\text{EL}}^{(i)}$ differs significantly from the EL cross section in the CDP approach $\sigma_{\text{EL}}^{(d)}$. Hence, two different sets of elastic scattering cross sections are produced in the present work for the symmetric collision system $\text{H} + \text{H}^+$ and compared to the results from [7, 13, 14, 16]. In terms of the phase shifts $\delta_{g,u}(l)$ the integral cross sections $\sigma_{\text{EL}}^{(i)}$ and $\sigma_{\text{EL}}^{(d)}$ in the QIP and CDP approaches, respectively, are as follows

Table 2 Phase shifts for $E_{c.m.}$ of 0.1 eV and 10 eV for representative values of l from the present fully quantal (QUANT), present semiclassical (JWKB), and obtained by quantal calculations of [10] (HK) and [13] (KS) where available.

	QUANT		JWKB		HK		KS	
	g	u	g	u	g	u	g	u
0.1 eV								
$l = 0$	1.221709	0.022883	1.22153	0.02799	1.234585	0.019202	1.21644	0.02638
$l = 5$	0.772645	0.624396	0.77276	0.62978	0.786002	0.620891	0.76734	0.62678
$l = 10$	3.303447	5.898259	3.30454	5.90441	3.317307	5.895139	3.29828	5.90031
$l = 20$	4.803677	5.473222	4.81175	5.48179	4.821474	5.471833	4.79954	5.47412
$l = 30$	0.572940	0.279244	0.57827	0.28236	0.574716	0.279115		
$l = 35$	0.279796	0.230648	0.28564	0.23139	0.280776	0.230459		
$l = 40$	0.173485	0.165080	0.17313	0.16517	0.175269	0.164588	0.17359	0.16505
$l = 60$	0.049876	0.049869	0.04985	0.04984	0.050337	0.050155	0.04990	0.04986
$l = 100$	0.010815	0.010815	0.01080	0.01080	0.010871	0.010871	0.01082	0.01081
10 eV								
$l = 0$	3.020760	3.347830	3.018120	3.345851	3.023478	3.332009	3.01732	3.35621
$l = 10$	2.237167	4.768027	2.235319	4.766228	2.239886	4.752823	2.23355	4.77620
$l = 20$	2.243118	3.299371	2.242186	3.297947	2.245989	3.285574	2.23933	3.30703
$l = 40$	0.127586	0.035456	0.127475	0.034722	0.131346	0.024905	0.12421	0.04172
$l = 100$	0.236404	0.854549	0.236683	0.854526	0.241409	0.850499	0.23642	0.85710
$l = 200$	0.502376	6.080151	0.502316	6.080164	0.502988	6.080018	0.50262	6.08038
$l = 300$	0.055114	0.028372	0.055085	0.028352	0.064165	0.037268	0.05512	0.02835

(see, e.g., Eqs. (80) and (97) in [11]):

$$\sigma_{\text{EL}}^{(i)} = \frac{\pi}{k^2} \left\{ \sum_{l=0}^{\text{even}} (2l+1) \left[\sin^2 \delta_g + 3 \sin^2 \delta_u \right] + \sum_{l=1}^{\text{odd}} (2l+1) \left[\sin^2 \delta_u + 3 \sin^2 \delta_g \right] \right\}, \quad (15)$$

$$\sigma_{\text{EL}}^{(d)} = \frac{\pi}{k^2} \left\{ \sum_l^{l_{\text{max}}} (2l+1) \left[\sin^2 \delta_g + \sin^2 \delta_u + 2 \sin \delta_g \sin \delta_u \cos(\delta_g - \delta_u) \right] \right\}. \quad (16)$$

The charge transfer (CDP picture) and spin exchange (QIP picture) integral cross sections are identical and computed by means of the equation

$$\sigma_{\text{CT}} = \frac{\pi}{k^2} \sum_{l=0}^{l_{\text{max}}} (2l+1) \sin^2(\delta_g - \delta_u). \quad (17)$$

To simplify the notation we drop the argument l of $\delta_{g,u}(l)$ in (15), (16), and (17). From here forward we use the subscript CT for either charge transfer or spin exchange. In the high energy limit the EL cross section in the QIP picture tends to the sum of the EL and CT cross sections in the CDP picture, $\sigma_{\text{EL}}^{(i)} = \sigma_{\text{EL}}^{(d)} + \sigma_{\text{CT}}$ [12–14].

3 Results

The very good agreement ($\sim 0.1\%$) of our calculations with the available results from [7] (see the supplement materials to that publication) has been obtained, except for

the narrow range of $E_{c.m.}$ from 2.2×10^{-4} to 2.8×10^{-4} eV, where our results differ from those of [7] by 2.5 – 8% (see Table 3).

Table 3 The total cross sections in atomic units ($a_0^2 = 2.8003 \times 10^{-17} \text{cm}^2$) for charge transfer (CT) and for elastic scattering in the distinguishable (ELd) and indistinguishable (ELi) particles approaches for representative $E_{c.m.}$ energies between 10^{-4} and 10^{-3} eV from the present work compared to the results from [7]. The numbers in parentheses denotes the powers of ten to be multiplied.

$E_{c.m.}$ (eV)	CT ¹	CT ²	ELd ¹	ELd ²	ELi ¹	ELi ²
1.000(-4)	4048.3	4047	7839.9	7832	10174.1	10179
1.096(-4)	3959.3	3958	8188.4	8176	10273.1	10270
1.202(-4)	4055.2	4054	8600.5	8582	10482.8	10470
1.349(-4)	4416.8	4415	8577.2	8560	10578.7	10570
1.549(-4)	4544.0	4546	7178.9	7167	9829.8	9816
1.778(-4)	4111.9	4114	5846.6	5819	8807.8	8781
1.950(-4)	3765.4	3765	5445.3	5398	8328.0	8288
2.089(-4)	3562.5	3548	5445.0	5359	8143.7	8076
2.188(-4)	3518.5	3471	5662.9	5517	8174.7	8060
2.399(-4)	4427.4	4068	6182.9	6266	8781.1	8624
2.692(-4)	3563.8	3739	3467.2	3532	6874.9	6976
3.090(-4)	2846.2	2895	3403.4	3344	6396.9	6373
3.467(-4)	2577.7	2605	3451.3	3397	6273.4	6242
4.571(-4)	2244.7	2256	3523.2	3487	6235.5	6210
5.248(-4)	2093.3	2100	3488.5	3462	6101.4	6081
6.026(-4)	1892.1	1895	3447.5	3429	5855.5	5840
6.918(-4)	1662.7	1663	3485.5	3473	5646.9	5635
8.128(-4)	1409.3	1408	3667.0	3659	5572.7	5563
9.772(-4)	1181.5	1178	3885.2	3885	5537.9	5533

¹present calculation

²Ref. [7]

For $E_{c.m.} = 10^{-4}$ eV the present elastic total cross section $\sigma_{EL}^{(i)}$ is 10174.09 a_0^2 compare to 10179.34 a_0^2 obtained in [7], for $E_{c.m.} = 10^{-1}$ eV this cross section is 782.564 a_0^2 compared to 783.0893 a_0^2 from [7].

Our calculated elastic and charge transfer integral cross sections over the center-of-mass energy range from 10^{-4} to 10^{-2} eV are displayed in Fig. 1, where we have included other theoretical results from [7, 9, 14]. Figure 2(a,b) shows the integral charge transfer cross section σ_{CT} from the present quantal and JWKB calculations for the energy range of 0.01 – 0.4 eV. Notice the oscillatory patterns in the cross section (at $E_{c.m.} \sim 0.127$ and 0.363 eV) not reported in previous studies. The inset to Fig. 2(a) shows a close-up of the sharp oscillation in the cross section at $E_{c.m.} \sim 0.127$ eV. The present results are compared with the theoretical data from [7, 9, 14, 16]. Our quantal calculations of the elastic scattering cross sections $\sigma_{EL}^{(i)}$ and $\sigma_{EL}^{(d)}$ are shown in Fig. 3 over the energy range from 0.01 to 10 eV. Comparison was made with the quantal calculations from [7, 14] and the JWKB calculations from [13]. Finally, the present results of the elastic scattering cross sections at ultra-low collision energies $10^{-10} \leq E_{c.m.} \leq 10^{-5}$ eV are displayed in Fig. 4 along with the calculations from

[5]. Clearly, for such low collision energies, the distinguishable particles approximation fails completely and ELd results are given only for comparison purposes.

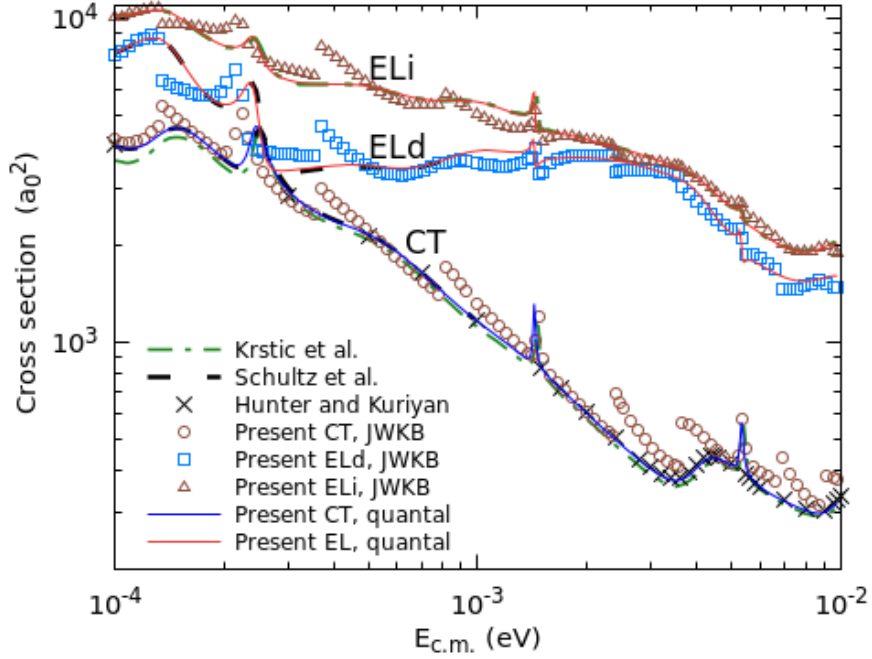


Fig. 1 Charge transfer (CT), elastic distinguishable (ELd), and elastic indistinguishable (ELi) integral cross sections from the present fully quantal (solid lines) and JWKB (symbols \circ , \square , and \triangle) calculations for center-of-mass collision energies within the range of 10^{-4} – 10^{-2} eV. Other theoretical results: $-\cdot-$, the σ_{CT} and $\sigma_{EL}^{(i)}$ calculations of Krstić *et al.* [14]; $- -$, the σ_{CT} and $\sigma_{EL}^{(d)}$ calculations of Schultz *et al.* [7]; \times , the σ_{CT} calculations of Hunter and Kuriyan [9]

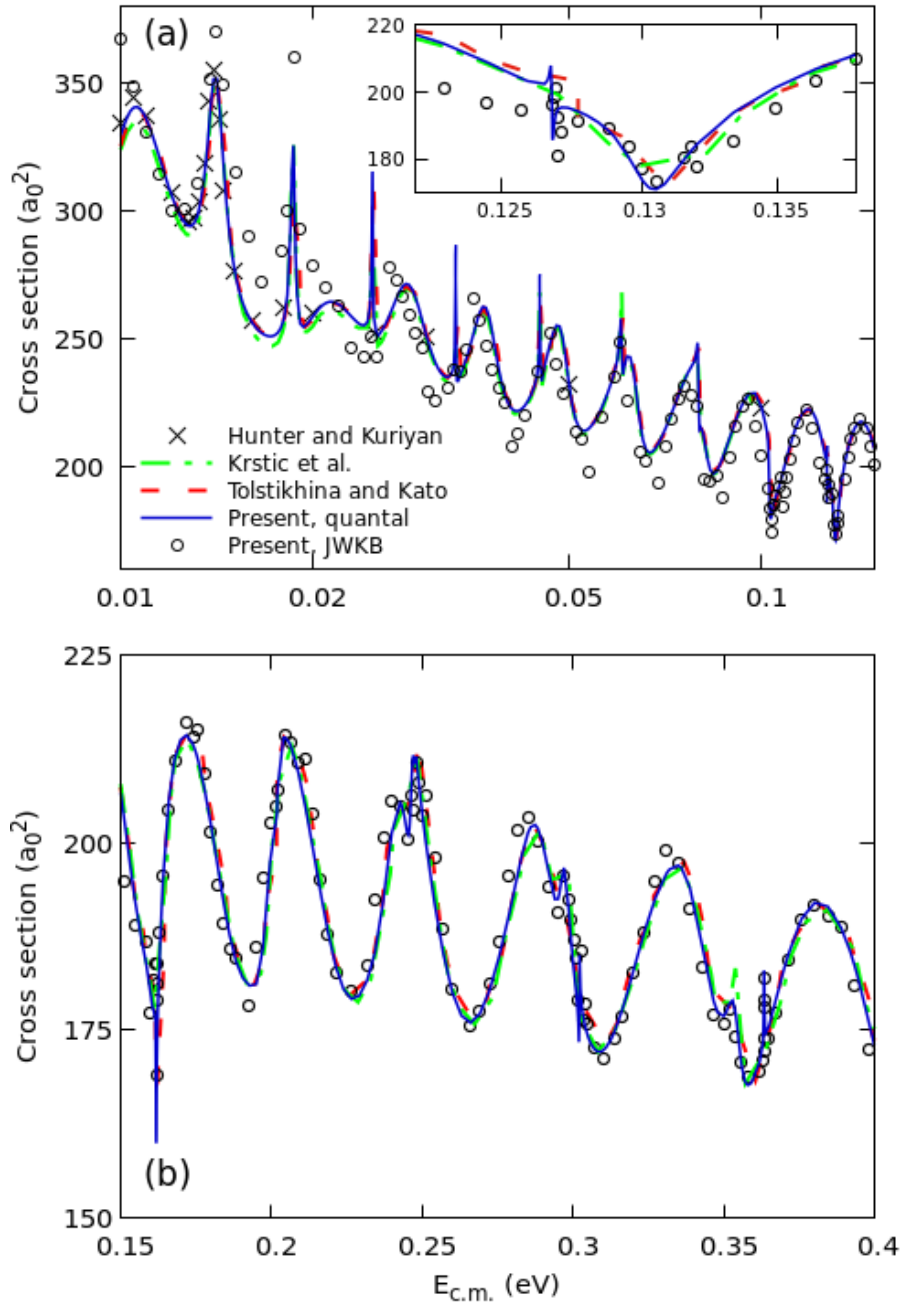


Fig. 2 (a) Charge transfer integral cross section from the present fully quantal (solid line) and JWKB (symbols \circ) calculations within the range of 0.01–0.15 eV. Other theoretical results: \times , [9]; $-\cdot-$, [14]; $- -$, [16]. The inset shows a close-up of the sharp oscillation at ~ 0.127 eV. (b) The same as in (a), except for the energy range of 0.15–0.4 eV

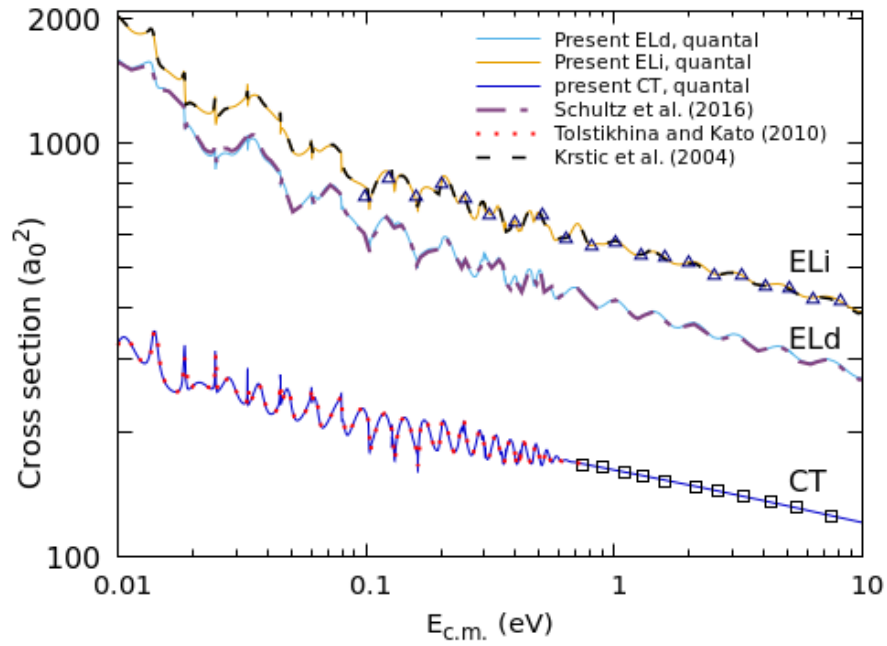


Fig. 3 Charge transfer (CT), elastic distinguishable (ELd), and elastic indistinguishable (ELi) integral cross sections for center-of-mass collision energies within the range of 0.01–10 eV. Solid lines, the present quantal calculations; — —, the quantal calculations from [7]; - - -, the quantal calculations from [14]; · · ·, the quantal calculations from [16]; \triangle and \square , the JWKB calculations for ELi and CT from [13]

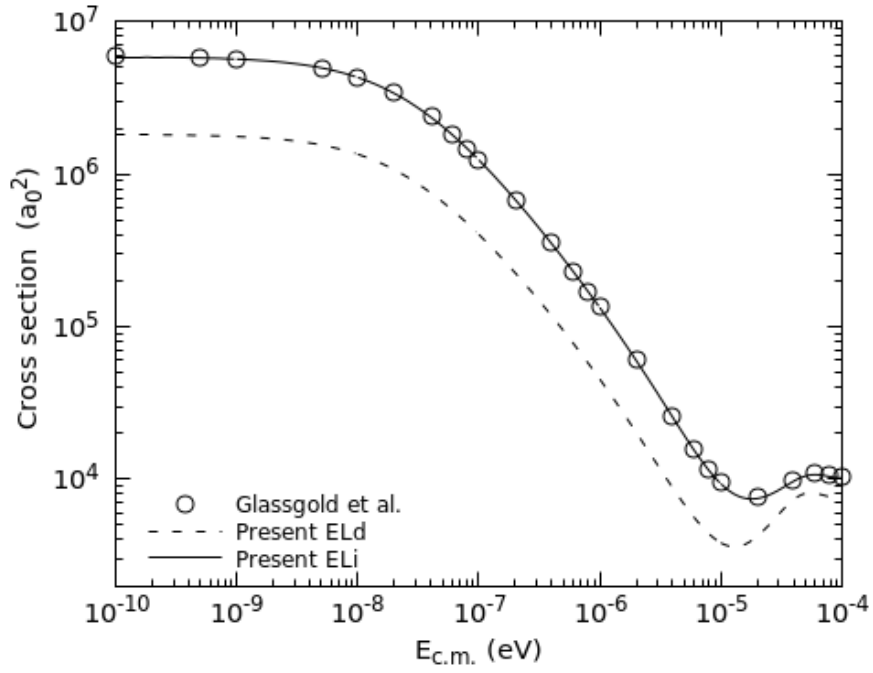


Fig. 4 Integral elastic cross sections for the energy range of 10^{-10} – 10^{-4} eV. Lines, the present calculations of $\sigma_{EL}^{(d)}$ and $\sigma_{EL}^{(i)}$; symbols \circ , the $\sigma_{EL}^{(i)}$ calculations from [5]

4 Discussion and concluding remarks

We have calculated the elastic and the resonant charge transfer cross sections in the collisions of proton with hydrogen atom H(1s). The calculations were performed over the range of the center-of-mass collision energies $10^{-10} - 10$ eV on a dense mesh of 1360 energy points. This allowed us to resolve all the known structures in the integral cross sections and to resolve the new ones at $E_{c.m.} \sim 0.127$ and 0.363 eV which were not reported in previous studies. For the computation of the scattering phase shifts (and consequently the integral cross sections), we used both the fully quantal and the JWKB methods. The agreement of the results obtained by these two methods is excellent for the energies $E_{c.m.} \gtrsim 0.47$ eV. For the energies $E_{c.m.} \lesssim 0.47$ eV the standard (one-turning-point) JWKB method is not applicable to the considered collision system, and the three-turning-point version of the method must be used instead. We find that JWKB describes the cross sections quite well, both qualitatively and quantitatively, down to the collision energies of ~ 0.01 eV. For even lower collision energies, the accuracy of JWKB method (as expected) decreases significantly, but it is still possible to obtain a reasonable estimate for the trend of the cross sections down to energies of 0.001 eV and even below.

To conclude, we have shown that properly using the semiclassical method for cross section calculation allows us to significantly expand the range of its application to very low collision energies. The obtained semiclassical results agree well with the fully quantal calculations and also reproduce correctly the oscillatory features in the integral cross sections of the reactions under consideration.

Acknowledgements. Author acknowledge the Visitors Program Fellowship from the Max Planck Institute for the Physics of Complex Systems (MPI-PKS) as well very grateful to MPI-PKS for their warm hospitality during the stay in Dresden. The comments of Dr. M. Eiles on a draft version are greatly appreciated. The major part of the computations were performed on the computer cluster in the Institute of Electron Physics (Uzhhorod). I thanks Prof. E. Remeta for many encouraging discussions and Dr. O. Papp for support with computing facilities. This study was partially supported by the U.S. Office of Naval Research Global (Grant N 62909-23-1-2088).

References

- [1] M.G. Santos, S.O. Kepler, Theoretical study of the line profiles of the hydrogen perturbed by collisions with protons. *Mon. Not. R. Astron. Soc.* **423**, 68–79 (2012) <https://doi.org/10.1111/j.1365-2966.2012.20631.x>
- [2] I. Pelisoli, M.G. Santos, S.O. Kepler, Unified line profiles for hydrogen perturbed by collisions with protons: satellites and asymmetries. *Mon. Not. R. Astron. Soc.* **448**, 2332–2343 (2015) <https://doi.org/10.1093/mnras/stv167>
- [3] D. Tselikhovich, C.M. Hirata, K. Heng, Excitation and charge transfer in H-H⁺ collisions at 5–80 keV and application to astrophysical shocks. *Mon. Not. R. Astron. Soc.* **422**, 2357–2371 (2012) <https://doi.org/10.1111/j.1365-2966.2012.20787.x>
- [4] R.R. Hodges, E.L. Breig, Ionosphere-exosphere coupling through charge exchange and momentum transfer in hydrogen-proton collisions. *J. Geophys. Res.* **96**, 7697–7708 (1991) <https://doi.org/10.1029/90JA02744>
- [5] A.E. Glassgold, P.S. Krstic, D.R. Schultz, H⁺ + H scattering and ambipolar diffusion heating. *Astrophys. J.* **621**, 808–816 (2005) <https://doi.org/10.1086/427686>
- [6] D.R. Schultz, P.S. Krstic, T.G. Lee, J.C. Raymond, Momentum transfer and viscosity from proton-hydrogen collisions relevant to shocks and other astrophysical environments. *Astrophys. J.* **678**, 950–960 (2008) <https://doi.org/10.1086/533579>
- [7] D.R. Schultz, S.Y. Ovchinnikov, P.C. Stancil, T. Zaman, Elastic, charge transfer, and related transport cross sections for proton impact of atomic hydrogen for astrophysical and laboratory plasma modeling. *J. Phys. B: At. Mol. Opt. Phys.* **49**, 084004 (2016) <https://doi.org/10.1088/0953-4075/49/8/084004>
- [8] N.D. Ciaratore, D.R. Schultz, Proton and hydrogen transport through hydrogen environments: Ionization and stripping. *The Astrophys. Journ. Suppl. Ser.* **252**, 7 (2021) <https://doi.org/10.3847/1538-4365/abc2c7>
- [9] G. Hunter, M. Kuriyan, Proton collisions with hydrogen atoms at low energies: Quantum theory and integrated cross-sections. *Proc. R. Soc. London, Ser. A* **353**, 575 (1977) <https://doi.org/10.1098/rspa.1977.0051>
- [10] G. Hunter, M. Kuriyan, Scattering of protons by hydrogen atoms at low energies. Phase shifts and differential cross sections. *At. Data Nucl. Data Tables* **25**, 287–310 (1980)
- [11] P.S. Krstić, D.R. Schultz, Elastic and related transport cross sections for collisions among isotopomers of H⁺ + H, H⁺ + H₂, H⁺ + He, H + H, and H + H₂. *At.*

- [12] P.S. Krstić, D.R. Schultz, Consistent definitions for, and relationships among, cross sections for elastic scattering of hydrogen ions, atoms, and molecules. *Phys. Rev. A* **60**, 2118 (1999) <https://doi.org/10.1103/PhysRevA.60.2118>
- [13] P.S. Krstić, D.R. Schultz, Elastic scattering and charge transfer in slow collisions: isotopes of H and H⁺ colliding with isotopes of H and with He. *J. Phys. B: At. Mol. Opt. Phys.* **32**, 3485–3509 (1999) <https://doi.org/10.1088/0953-4075/32/14/317>
- [14] P.S. Krstić, J.H. Macek, S.Y. Ovchinnikov, D.R. Schultz, Analysis of structures in the cross sections for elastic scattering and spin exchange in low-energy H⁺ + H collisions. *Phys. Rev. A* **70**, 042711 (2004) <https://doi.org/10.1103/PhysRevA.70.042711>
- [15] M. Li, B. Gao, Proton-hydrogen collisions at low temperatures. *Phys. Rev. A* **91**, 032702 (2015) <https://doi.org/10.1103/PhysRevA.91.032702>
- [16] I.Y. Tolstikhina, D. Kato, Resonance charge exchange between excited states in slow proton-hydrogen collisions. *Phys. Rev. A* **82**, 032707 (2010) <https://doi.org/10.1103/PhysRevA.82.032707>
- [17] A. Dalgarno, H.N. Yadav, Electron capture II: Resonance capture from hydrogen atoms by slow protons. *Proc. Phys. Soc. A* **66**, 173 (1953) <https://doi.org/10.1088/0370-1298/66/2/308>
- [18] H. Nakamura, Semiclassical approach to charge-transfer processes in ion-molecule collisions. In: M. Baer, C.-Y. Ng (eds.) *State-selected and State-to-state Ion-molecule Reaction Dynamics. Part 2. Theory*, vol. 82, pp. 243–319. Wiley, New York (1992). <https://doi.org/10.1002/9780470141403.ch5>
- [19] K.E. Thylwe, A. Bárány, A semiclassical analysis of orbiting resonances in slow charge transfer processes. *Nucl. Instr. Meth. Phys Res. B.* **9**, 435–437 (1985) [https://doi.org/10.1016/0168-583X\(85\)90342-8](https://doi.org/10.1016/0168-583X(85)90342-8)
- [20] J.N.L. Connor, On the semi-classical description of molecular orbiting collisions. *Mol. Phys.* **15**, 621–631 (1968) <https://doi.org/10.1080/00268976800101521>
- [21] J.N.L. Connor, Semiclassical theory of elastic scattering. In: M.S. Child (ed.) *Semiclassical Methods in Molecular Scattering and Spectroscopy*, pp. 45–107. D. Reidel Publishing, Dordrecht (1980) <https://doi.org/10.1007/978-94-009-8996-2>
- [22] H.J. Korsch, K.E. Thylwe, Orbiting and rainbow structures in low-energy elastic differential cross sections. *J. Phys. B: At. Mol. Opt. Phys.* **16**, 793–815 (1983) <https://doi.org/10.1088/0022-3700/16/5/013>

- [23] P.J. Mohr, D.B. Newell, B.N. Taylor, Codata recommended values of the fundamental physical constants: 2014. *Rev. Mod. Phys.* **88**, 035009 (2016) <https://doi.org/10.1103/RevModPhys.88.035009>
- [24] H. Wei, R.J. Le-Roy, Calculation of absolute scattering phase shifts. *Mol. Phys.* **104**, 147–150 (2006) <https://doi.org/10.1080/00268970500302410>
- [25] J.M. Thijssen, *Numerical Physics*. Cambridge University Press, Cambridge (1999)
- [26] P. Gianozzi, *Numerical Methods in Quantum Mechanics*. Lecture notes, 2021, <https://www.fisica.uniud.it/~giannozz/Corsi/MQ/LectureNotes/mq.pdf>
Accessed 6 February 2025